

Pyrolysis kinetic analysis of sequential extract residues from Hefeng sub-bituminous coal based on Coats-Redfern method

Xian-Jin Huang

Wen-Long Mo (✉ mowenlong@xju.edu.cn)

Xinjiang University

Ya-Ya Ma

Xinjiang University

Xiao-Qiang He

Xinjiang University

Yelixiati Syls

Xinjiang University

Xian-Yong Wei

China University of Mining and Technology

Xing Fan

Shandong University of Science and Technology

Xiao-Qin Yang

Xinjiang Yihua Chemical Industry Co., Ltd

Shu-Pei Zhang

Xinjiang Yihua Chemical Industry Co., Ltd

Research Article

Keywords: Extract residues, Pyrolysis, Coats-Redfern method, Kinetic analysis

Posted Date: November 30th, 2021

DOI: <https://doi.org/10.21203/rs.3.rs-1109976/v1>

License: © ⓘ This work is licensed under a Creative Commons Attribution 4.0 International License.

[Read Full License](#)

1 **Pyrolysis kinetic analysis of sequential extract residues from Hefeng**
2 **subbituminous coal based on Coats-Redfern method**

3 Xian-Jin Huang¹, Wen-Long Mo^{*1}, Ya-Ya Ma¹, Xiao-Qiang He¹, Yelixiati·Syls¹, Xian-Yong
4 Wei^{*1,2}, Xing Fan^{1,3}, Xiao-Qin Yang⁴, Shu-Pei Zhang⁴

5 *1. State Key Laboratory of Chemistry and Utilization of Carbon-Based Energy*
6 *Resources and Key Laboratory of Coal Clean Conversion & Chemical Engineering*
7 *Process (Xinjiang Uyghur Autonomous Region), College of Chemical Engineering,*
8 *Xinjiang University, Urumqi, Xinjiang 830046, China.*

9 *2. Key Laboratory of Coal Processing and Efficient Utilization, Ministry of Education,*
10 *China University of Mining & Technology, Xuzhou 221116, Jiangsu, China.*

11 *3. College of Chemical and Biological Engineering, Shandong University of Science*
12 *and Technology, Qingdao, Shandong 266590, China.*

13 *4. Xinjiang Yihua Chemical Industry Co., Ltd., Changji 831700, China.*

14 **Abstract:** Sequential extract residues (R_i , $i=1, 2, 3, 4, 5$) were obtained from Hefeng
15 acid-washing coal (HFAC) by petroleum ether, carbon disulfide, methanol, acetone
16 and isometric carbon disulfide/acetone mixture, sequentially. Pyrolysis behavior of
17 the samples was carried out using thermogravimetry analysis. Coats-Redfern method
18 with different reaction order was used to analyze the pyrolysis kinetic of each sample,
19 and the kinetic parameters, including correlation coefficient (R^2), activation energy
20 (E), pre-exponential factor (A), were calculated. Results showed that the weight loss
21 of extract residues was higher than HFAC, and pyrolysis behavior varies greatly for
22 residues, which may be due to unstable structure after extraction. From conversion-
23 temperature (α - T) curves, pyrolysis process was divided into three stages: low-
24 temperature stage (150-350 °C), medium temperature stage (350-550 °C) and high
25 temperature stage (550-950 °C). And the medium temperature stage made great

26 contribution to the process of pyrolysis, which was dominated by depolymerization
27 and decomposition reaction, and the effect of kinetic fitting to this stage is better, with
28 R^2 higher than 0.95. Relationship between kinetic parameters and reaction order
29 showed that swelling effect might be an important reason for the discrepancy of E for
30 each sample in the process of pyrolysis. And $\ln(A)$ - E relationship has a great
31 significance to predict E and the A under higher reaction order.

32 **Key words:** Extract residues; Pyrolysis; Coats-Redfern method; Kinetic analysis

33 Corresponding author: Wen-Long Mo, E-mail: mowenlong@xju.edu.cn

34 Xian-Yong Wei, E-mail: wei_xianyong@163.com

35 **1. Introduction**

36 In recent years, increasing consumption of coal, the main energy source in China,
37 has caused serious environmental pollution problems. However, coal still play a
38 leading role in Chinese primary energy consumption for a long time in the future.
39 Therefore, clean and efficient utilization of coal has become the top priority [1-4].
40 Solvent extraction under mild conditions can separate organic matter from coal by the
41 principle of similar phase dissolution, without damaging the environment, and the
42 structure and composition characteristics of coal can be reflected by analyzing the
43 molecular structure characteristics of the soluble molecules [5-6]. There are five kinds
44 of intermolecular forces in coal, including entanglement interaction between alkyl and
45 alkyl groups, π - π interaction between aromatic rings, weak hydrogen bond, strong
46 hydrogen bond and hydrogen bond/ π - π complex interaction. Different solvent can
47 selectively destroy the intermolecular interaction in low-rank coal [7-9]. Therefore,
48 sequential extraction with different solvent can effectively improve the extraction
49 efficiency of organic matter in coal.

50 Macro-kinetics is widely used in study of coal pyrolysis characteristics and reaction

51 mechanism, which shows high theoretical and practical significance for improving
52 clean and efficient utilization of coal [10-11]. Thermogravimetric analysis (TGA) is a
53 kind of thermal analysis technology, which measures the change of material quality
54 with temperature and time in a controlled environment. This method has a lot of
55 advantages, such as simple pretreatment, no reagent and application [12-13]. By the
56 establishment of kinetic model, pyrolysis process of coal can be quantitatively
57 analyzed, which is convenient to understand the pyrolysis characteristics and
58 mechanism of coal. Many theoretical models, including zero-order empirical model,
59 single reaction model, multi-stage reaction model and distributed activation energy
60 model (DAEM), have been put forward by researchers. In addition, many methods for
61 calculating kinetic parameters are proposed according to the above model, including
62 Coats-Redfern method, Kissinger method, Dzawa method and Doyle method.
63 However, a universal model and method has not been developed due to the
64 complexity and difference of coal structure. Among them, single reaction model,
65 which considered the process of coal pyrolysis as an approximately first-order or n-
66 order reaction and can well predict the kinetic parameters, has been widely concerned
67 [14].

68 Liu et al. [15] investigated the effect of coal particle size on pyrolysis performance
69 by Coats-Redfern method. It was found that the smaller the coal particle size is, the
70 faster the surface heating rate, resulting in higher heat flux and lower activation
71 energy. In addition, with the decrease of particle size, the specific surface area
72 increased significantly, and the active sites increased, which could promote the release
73 of primary pyrolysis products. According to TGA, Geng et al. [16] discussed the
74 behavior of kinetics using Shenmu bituminous coal and its pyrolysis products. It was
75 found that pyrolysis process involved many types of covalent and other chemical

76 bonds, resulting that cleavage of each bond need different activation energies. Du et al.
77 [17] reported the pyrolysis kinetics of Shenfu coal, and divided the pyrolysis process
78 into three stages. Low temperature stage was contributed by small molecules of gas
79 and water. In the middle temperature region, a large amount of gas and tar vapors
80 were evaporated, with semi-coke and coke formed in the process. And volume
81 shrinkage could be observed in the high temperature range. Wu et al. [18] used n -level
82 single reaction model to analyze the pyrolysis characteristics of Xinjiang bituminous
83 coal. It was found that wonderful effect can be obtained in the violent pyrolysis stage
84 when the reaction order $n=2$, and the reaction order $n=1$ is suitable for the
85 polycondensation and secondary cracking stage.

86 In this paper, pyrolysis kinetics of Xinjiang Hefeng acid-washing coal (HF_{AC}) and
87 its sequential extract residues from petroleum ether (PE), carbon disulfide (CDS),
88 methanol (M), acetone and isometric acetone/carbon disulfide (IMCDSAM) was
89 discussed under the reaction order of $n=1-5$ with single reaction model by Coats-
90 Redfern method. And the structure and pyrolysis characteristics of the samples were
91 also investigated according to the kinetics parameters.

92 **2. Experimental**

93 **2.1. Coal sample**

94 The used subbituminous coal sample was selected from Hefeng, Xinjiang, China.
95 **Table 1** shows the proximate and ultimate analyses of Hefeng coal (HF) and its acid-
96 washing sample by hydrochloric acid and hydrofluoric acid.

97 It can be seen from **Table 1**, that HF shows the characteristics of high ash, high
98 volatile matter, high ratio of hydrogen carbon and low sulfur. After acid-washing
99 treatment, the ash content in HF_{AC} is greatly reduced, from 21.18% to 1.84%, with the
100 removal rate high of 91.31%, indicating that acid-washing can effectively remove ash

101 in coal, thus we can study the pyrolysis characteristics of organic matter in coal, and
102 the effect of ash can be ignored.

103 **2.2. Sequential extraction process**

104 The detailed process of aid-washing can be known from our group previous
105 references [19,20]. HF_{AC} was successively extracted with petroleum ether (PE),
106 carbon disulfide (CDS), methanol (*M*), acetone and isometric acetone/carbon disulfide
107 (IMCDSAM) by ultrasonic assisted five-stage extraction. Residues obtained from
108 each stage were recorded as R_i (i=1, 2, 3, 4, 5), and sequential extraction process is
109 shown in **Fig. 1**. The yield, structural characteristics and composition distribution of
110 the extract have been described in the literature [21].

111 **2.3. Thermogravimetric analysis (TGA)**

112 With N₂ as carrier gas, the pyrolysis behavior of HF_{AC} and R_i (i=1, 2, 3, 4, 5) was
113 carried out on a thermogravimetric analyzer SDT-Q600 from TA company. The
114 temperature is raised from ambient to 1000 °C, with heating rate of 10 °C/min.

115 **2.4. Pyrolysis kinetics analysis**

116 The pyrolysis kinetics of each sample was studied by conversion and other
117 parameters. In this experiment, Coats-Redfern method was used to calculate the
118 kinetics parameters for the process of pyrolysis with a single heating rate.

119 According to Coats-Redfern method, it generally has the following expression:

120 when $n=1$:

$$121 \quad \ln \left[-\frac{\ln(1-\alpha)}{T^2} \right] = \ln \left[\frac{AR}{\phi E} \left(1 - \frac{2RT}{E} \right) \right] - \frac{E}{RT} \quad (1)$$

122 when $n \neq 1$:

$$123 \quad \ln \left[\frac{1 - (1-\alpha)^{1-n}}{T^2(1-n)} \right] = \ln \left[\frac{AR}{\phi E} \left(1 - \frac{2RT}{E} \right) \right] - \frac{E}{RT} \quad (2)$$

124 where α is the conversion; n is the reaction order; E is the activation energy, kJ/mol; T

125 is the kelvin temperature, K; ϕ is the heating rate, K/min; R is the constant, 8.314
126 J/(mol·K); A is the pre-exponential factor, min⁻¹.

127 According to the thermogravimetric analysis, the conversion is expressed as
128 follows:

$$129 \quad \alpha = \frac{m_0 - m_g}{m_0 - m_f}$$

130 where m_g is the mass of sample at a certain time (or temperature), mg; m_0 is the initial
131 mass of sample, mg; m_f is the ending mass of sample reaction, mg.

132 The equations (1) and (2) are analyzed. Generally, for most reaction temperature
133 regions and most E, the term of $E/RT \geq 1$, $2RT/E \rightarrow 0$. Hence, $(1 - 2RT/E) \approx 1$, then
134 equations (1) and (2) can be simplified as follows:

$$135 \quad \ln \left[-\frac{\ln(1-\alpha)}{T^2} \right] = \ln \left(\frac{AR}{\phi E} \right) - \frac{E}{RT} \quad (3)$$

$$136 \quad \ln \left[\frac{1 - (1-\alpha)^{1-n}}{T^2(1-n)} \right] = \ln \left(\frac{AR}{\phi E} \right) - \frac{E}{RT} \quad (4)$$

137 When $n = 1$, let $y = \ln \left[-\frac{\ln(1-\alpha)}{T^2} \right]$; when $n \neq 1$, let $y = \ln \left[\frac{1 - (1-\alpha)^{1-n}}{T^2(1-n)} \right]$; let $x = \frac{1}{T}$.

138 When n takes different reaction orders and plot y against x , and the regression
139 equation is carried out, with the slope of $-E/R$ and the intercept of $\ln(AR/\phi E)$.
140 Activation energy and pre-exponential factor of the reaction can be calculated
141 according to the regression equation.

142 3. Results and discussion

143 3.1. TG analysis

144 **Fig. 2** shows TG and DTG profiles of Hefeng acid-washing coal and its extract
145 residues. It can be seen from **Fig. 2 (a)** that there are significant differences in TG
146 profiles to the samples. The weight loss of HF_{AC} is smaller of 41.03%. TG profiles of

147 R₁ and R₂ are basically the same, with weight loss of 54.97% and 55.02%,
148 respectively. TG profiles of R₃, R₄ and R₅ are similar, with weight loss of 42.33%,
149 44.92% and 42.53%, respectively. When temperature is lower than 350 °C, the weight
150 loss of each sample shows little difference, with the value about 10%. This stage is
151 mainly ascribed to the desorption and decarboxylation of adsorbed water and small
152 molecule gases, and the weight loss accounts for 18%-25% of the total pyrolysis
153 process. In addition, it is not difficult to see that the weight loss of the residues was
154 larger than that of HF_{AC}, which might be derived from that, after solvent extraction,
155 the molecular structure of coal is unstable and some solvents were remained in the
156 residues. Temperature from 350 °C to 550 °C is the main thermal decomposition stage,
157 which may be belonged to depolymerization and decomposition of larger molecular
158 structure in coal, accompanied by polycondensation reaction to generate some gases
159 (methane and its homologues, olefins, water, etc.).

160 It can be seen from DTG diagram in **Fig. 2 (b)** that the weight loss rate of R₁ and
161 R₂ is smaller than that of HF_{AC}. This may be due to the fact that volatile substances
162 are dissolved into the extractant after primary and secondary solvent extraction, which
163 might be leading to the molecular skeleton structure is more stable. Moreover, some
164 solvents may enter into the pores of coal molecular structure to form surface tension,
165 which makes pyrolysis process more difficult. While the weight loss rate of R₃, R₄
166 and R₅, from DTG profiles, is larger than that of HF_{AC}, which might be due to the
167 influence of swelling on the molecular structure of coal after many times solvent
168 extraction, and the volume expansion might be taken place to accelerate the process of
169 pyrolysis [22]. When temperature is higher than 550 °C, aromatic substances
170 condense, and aromatic nuclei increase, and semi-coke forms coke rock. The weight
171 loss of R₁ and R₂ is the largest in this stage. This may be due to the polycondensation

172 reaction between residual solvents and substances in the residues, releasing a large
173 amount of small molecular gases. The reason for the small weight loss of R₃, R₄ and
174 R₅ might be concluded that the macromolecular channels formed by swelling under
175 high temperature rapidly collapse and agglomerate to produce molecules.

176 It can also be seen from the DTG profiles that there are two weight loss rate peaks.
177 The first weight loss rate peak appeared at about 100 °C, corresponding to the
178 evaporation of water and small molecular gases; the second weight loss rate peak is
179 larger, appearing in the between of 400-500 °C. This range is the main stage of the
180 pyrolysis reaction, and more substances in the sample were depolymerized and small
181 molecular gases were released. It can be seen that the peak value of weight loss rate of
182 R₁ and R₂ is small of -0.14% ·°C⁻¹. The peak value of weight loss rate of R₃, R₄, R₅
183 and HF_{AC} are almost the same, and that of R₄ is larger of -0.22%·°C⁻¹.

184 **3.2. Conversion-temperature diagram**

185 **Fig. 3 (a)** shows the relationship between pyrolysis conversion and temperature of
186 Hefeng acid-washing coal and the corresponding extract residues. It can be seen that
187 there is little difference for the conversion-temperature profiles of the acid-washing
188 coal and its extract residues. Combined TG-DTG profiles with α -*T* diagram, pyrolysis
189 process can be divided into three stages [23-25], as shown in **Fig. 3 (b)**. The samples
190 contain a small amount of moisture, so the weight loss below 150 °C is taken as the
191 initial pyrolysis process. The intersection points A of tangent line of TG and DTG
192 profile is taken as the dividing temperature point of the first stage (S1, 150-350 °C)
193 and B as the second stage (S2, 350-550 °C), and the third stage (S3) is ranged from
194 550-950 °C. It can be seen from **Fig. 3 (a)** that the change trend of conversion profiles
195 is basically consistent in the stage of 150-350 °C. And the conversions of extract
196 residues are higher than that of acid-washing coal, which may be due to the

197 desorption of more small molecules in this stage (**Fig. 2 (a)**). In the stage of 350-550
198 °C, the conversions increase rapidly, which may be due to that this temperature region
199 is the main stage of pyrolysis reaction, and a large number of substances are
200 depolymerized and decomposed. Moreover, the conversion profiles are divergent in
201 this temperature range, that is the increasing trend of the conversion of R₃, R₄, R₅ and
202 HF_{AC} is more obvious. In the stage of 550-950 °C, the conversion of R₃, R₄, R₅ and
203 HF_{AC} increases slowly, indicating that the pyrolysis process becomes gentle. The
204 result may be caused from that the main reaction in this stage is polycondensation,
205 which is difficult to take place.

206 **3.3. Coats-Redfern kinetic analysis**

207 In order to discuss the pyrolysis kinetic characteristics of the samples, kinetic
208 fitting of each sample in the temperature range of 350-550 °C was carried out by
209 Coats-Redfern method, and the fitting diagram of reaction order $n=0.5-5$ was obtained,
210 as shown in **Fig. 4**. It can be seen that each reaction order has little effect on R₁ and
211 R₂, which may be due to the samples have a stable and similar main structure. And
212 our previous work [19] showed that extraction process has an effective effect to
213 organic matter, while does not change the main structure of coal. The fitting curves of
214 R₃, R₄, R₅ and HF_{AC} have a large deviation when $n=3$, indicating that different
215 reaction order can obviously affect the fitting effect. And this phenomenon needs to
216 be further explored from the pyrolysis reaction mechanism.

217 **3.4. Calculation of kinetic parameters**

218 According to the fitting curves, the kinetic parameters, including regression
219 equation (y), correlation coefficient (R^2), activation energy (E), pre-exponential factor
220 (A), were calculated under different reaction orders by Coats-Redfern method. Results
221 were shown in **Table 2**.

222 It can be seen that the values of R^2 are above 0.9500, indicating that the fitting
223 correlation of each sample is better. Activation energy can reflect the difficulty of
224 pyrolysis reaction. It is not difficult to see that the variation for activation energy is
225 very large after extraction. Residues had lower activation energy than HF_{AC},
226 indicating that coal after extraction more conducive to pyrolysis. Pre-exponential
227 factor is a constant determined by the nature of the reaction. The value of A varies
228 greatly in different reaction order. Many studies [25-27] have found that the pre-
229 exponential factor has great difference under different reaction conditions. The value
230 of A increases with the increase of heating rate and reaction order, and it is also found
231 that there is a "compensation effect" between activation energy and pre-exponential
232 factor. Coats-Redfern integral formula assumes that the term E/RT is far greater than 1,
233 that is, $2RT/E \rightarrow 0$. Therefore, the smaller the $2RT/E$ value, the better the calculation
234 results of kinetic parameters can meet the preconditions of the formula.

235 **3.5. Relationship between kinetic parameters and reaction order**

236 Pyrolysis is a macroscopic process, and kinetic parameters can reflect the
237 comprehensive performance of pyrolysis process. The higher the reaction order, the
238 more complex the pyrolysis process. The relationship between kinetic parameters and
239 reaction order in the temperature range of 350-550 °C is shown in **Fig. 5**.

240 **Fig. 5(a)** shows the relationship between activation energy and reaction order. It
241 can be seen from **Fig. 5(a)** that activation energy increases with the increases of
242 reaction order for each sample, indicating that the higher the reaction order, the more
243 complex the pyrolysis reaction might be. While activation energy presents significant
244 difference for HF_{AC} and its residues, which could be related to the composition
245 difference of each sample after sequential extraction. Ma et al. [28] found that coal
246 sample showed swelling effect in solvent, which is a process of gradual expansion,

247 micro-explosion, pore collapse and formation of fragments, and swelling coefficient
248 with different solvent varies greatly. After the process of ultrasonic-assisted sequential
249 extraction, with pore structure of coal sample collapse, with weak bridge bond
250 destroyed and cross-linked network structure slacked, the extract residues could be
251 swelled under different solvents. Therefore, swelling effect might be an important
252 reason for the discrepancy of activation energy for each sample in the process of
253 pyrolysis.

254 **Fig. 5 (b)** shows the relationship between correlation coefficient R^2 and reaction
255 order. The values of R^2 were all above 0.95, indicating that the correlation effect was
256 acceptable. Correlation coefficient R^2 increases firstly and then decreases with the
257 reaction order, and the value of HF_{AC} reaches the maximum of 0.972 when the
258 reaction order $n=2$, while the values of all the residues reach the maximum when
259 reaction order $n=1.5$, indicating that kinetic parameters show more accuracy when
260 reaction order $n=1.5-2$.

261 **Fig. 5 (c)** shows the relationship between $2RT/E$ and reaction order. $2RT/E \rightarrow 0$ is
262 the precondition for the calculation of kinetic parameters for Coats-Redfern method.
263 The lower the value, the higher the reliability of the model is. It can be seen that the
264 value of $2RT/E$ decreases with the increase of reaction order, indicating that high
265 reaction order can better meet the condition of Coats-Redfern method.

266 Literatures ^[29-31] found that pre-exponential factor increases when activation energy
267 increases, and the factor decreases when the activation energy decreases, which is
268 called “dynamic compensation effect”. Meng et al. ^[32] also discovered that there was
269 “dynamic compensation effect” between activation energy and pre-exponential factor
270 in the process of coal gasification, and the gas diffusion has a significant impact on
271 the compensation effect.

272 The “dynamic compensation effect” can be expressed by mathematical formula as
273 follows:

$$274 \quad \ln(A) = qE + p^{[33]}$$

275 Where q and p are the compensation parameters.

276 In order to further explore the compensation effect of activation energy and pre-
277 exponential factor, the diagram of $\ln(A)$ - E is plotted, and the profiles are shown in
278 **Fig. 5(d)**. It can be found that the relationship between activation energy and pre-
279 exponential factor is almost a line. And there is a one-to-one correspondence between
280 the activation energy and the reaction order, which could be used to predict the
281 activation energy and the pre-exponential factor under higher reaction order.

282 **4. Conclusions**

283 In this paper, thermogravimetric analyses of acid-washing coal and its extract
284 residues were carried out. Results showed that the weight losses of all stages for
285 extract residues were higher than that of HFAC. Coats-Redfern method was used to fit
286 the pyrolysis kinetics under the reaction order of $n=0.5-5$ at different temperature
287 stages, and the kinetic parameters were calculated according to the fitting curves.
288 Results showed that, in the medium temperature range, the correlation coefficient R^2
289 is larger, and the fitting effect is better. Relationship between kinetic parameters and
290 reaction order showed that swelling effect might be an important reason for the
291 discrepancy of activation energy for each sample in the process of pyrolysis, and that
292 high reaction order can better meet the condition of Coats-Redfern method. And
293 $\ln(A)$ - E relationship can be used to predict the activation energy and the pre-
294 exponential factor under higher reaction order.

295 **Acknowledgements**

296 This work was supported by the Tianchi project for introducing high-level talents to

297 Xinjiang Uyghur Autonomous Region (China), Key Laboratory of Coal Processing
298 and Efficient Utilization from Ministry of Education and Open Project of Key
299 Laboratory of Xinjiang Uygur Autonomous Region (Grant 2018D04008).

300 **References**

301 [1] Tahmasebi A, Yu J, Han Y, Yin F, Bhattacharya S, Stokie D. Study of chemical
302 structure changes of Chinese lignite upon drying in superheated steam, microwave,
303 and hot air[J]. *Energy Fuels*, 2012, 26(6):3651-60.

304 [2] Kong J, Wei XY, Li ZK, Yan HL, Zhao MX, Zong ZM. Identification of
305 organonitrogen and organooxygen compounds in the extraction residue from
306 Buliangou subbituminous coal by FTICRMS[J]. *Fuel*, 2016, 171:151-158.

307 [3] Liu FJ, Zong ZM, Li WT, et al. A three-step dissociation method for converting
308 Xiaolongtan lignite into soluble organic compounds: Insights into chemicals,
309 geochemical clues, and structural characteristics[J]. *Fuel*, 2018,242(242):883-892.

310 [4] He XQ, Mo WL, Wang Q, Ma YY, Ma FY, Fan X, Wei XY. Effect of swelling
311 treatment by organic solvent on the structure and pyrolysis performance of the direct
312 coal liquefaction residue[J]. *Energy & Fuels*, 2020, 34(7): 8685-8696.

313 [5] Lei Z, Zhang Y, Wu L, et al. The dissolution of lignite in ionic liquids[J]. *RSC*
314 *Advances*, 2013, 3(7): 2385-2389.

315 [6] Liu F J, Wei X Y, Xie R L, Wang Y G, Li W T, Li Z K, et al. Characterization of
316 oxygencontaining species in methanolysis products of the extraction residue from
317 Xianfeng lignite with negative-ion electrospray ionization Fourier transform ion
318 cyclotron resonance mass spectrometry[J]. *Energy Fuels*, 2014, 28:5596-605.

319 [7] Hu R N, Wang Z C, Li L, Wang X L, Shui H F, et al. Effect of solvent extraction
320 pretreatments on the variation of macromolecular structure of low rank coals [J].
321 *Journal of Fuel Chemistry and Technology*, 2018, 46(7): 778-786.

- 322 [8] Lv JH, Wei XY, Wang YH, et al. Mass spectrometric analyses of biomarkers and
323 oxygen-containing species in petroleum ether-extractable portions from two Chinese
324 coals[J]. Fuel, 2016, 173:260-267.
- 325 [9] Shui H, Zhou Y, Li H, et al. Thermal dissolution of Shenfu coal in different
326 solvents[J]. Fuel, 2013, 108:385-390.
- 327 [10] Heydari M, Rahman M, Gupta R. Kinetic study and thermal decomposition
328 behavior of lignite coal [J]. International Journal of Chemical Engineering, 2015,1-9.
- 329 [11] Song HJ, Liu GR, Zhang JZ, et al. Pyrolysis characteristics and kinetics of low
330 rank coals by TG-FTIR method [J]. Fuel Processing Technology, 2017, 156: 454-460.
- 331 [12] Guo YH, Cheng F. Adaptability Analysis of Kinetic Model of Blended Coal
332 Pyrolysis[J]. Journal of Combustion Science and Technology, 2019, 25(6): 509-518.
- 333 [13] Wu D, Liu GJ, Sun RY. Investigation on structural and thermodynamic
334 characteristics of perhydrous bituminous coal by Fourier transform infrared
335 spectroscopy and thermogravimetry/mass spectrometry[J]. Energy Fuels 2014,
336 28:3024-3035.
- 337 [14] W. de Jong, G. Di Nola, B.C.H. Venneker, H. Spliethoff, M.A. Wójtowicz. TG-
338 FTIR pyrolysis of coal and secondary biomass fuels: determination of pyrolysis
339 kinetic parameters for main species and NO_x precursors[J]. Fuel, 2007, 86(15):2367-
340 2376.
- 341 [15] Liu JX, Ma JF, Luo L, et al. Pyrolysis of superfine pulverized coal. part 5.
342 thermogravimetric analysis[J]. Energy Conversion and Management, 2017, 154:491-
343 502.
- 344 [16] Geng CC, SY Li, Yue CT, Ma Y. Pyrolysis characteristics of bituminous coal[J].
345 Elsevier Ltd,2016,89(4):1-6.
- 346 [17] Du RL, Wu K, Zhang L, et al. Thermal behavior and kinetic study on the

347 pyrolysis of Shenfu coal by sectioning method[J]. Journal of Thermal Analysis and
348 Calorimetry; 2016, 125(2):959-966.

349 [18] Wu F, Wang MH. Research on the pyrolysis characteristic and kinetics of
350 Xinjiang bituminous coals[J]. China Coal, 2019,45(02):84-90+95.

351 [19] Ma YY, Ma FY, Mo WL, Wang Q. Five-stage sequential extraction of Hefeng
352 coal and direct liquefaction performance of the extraction residue[J]. Fuel, 2020, 266,
353 117039-117048.

354 [20] Wang Y, Ma YY, Mo WL, Gong WT, Ma FY, Fan X, Wei XY,
355 Zhang SP. Functional groups of sequential extracts and corresponding residues from
356 Hefeng sub-bituminous coal based on FT-IR analysis[J]. Journal of Fuel Chemistry
357 and Technology ,2021, 21, 1-12.

358 [21] Sarwar A, Khan M N, Azhar K F. Kinetic studies of pyrolysis and combustion of
359 Thar coal by thermogravimetry and chemometric data analysis[J]. Journal of Thermal
360 Analysis and Calorimetry, 2012, 109(1): 97-103.

361 [22] Ma YY, Wang HH, Mo WL, Zhang XY, et al. Effect of swelling by organic
362 solvent on structure, pyrolysis and methanol extraction performance of Hefeng
363 bituminous Coal [J]. ACS Omega, 2021, 6(23): 14765-14773.

364 [23] Liu QH, Wu K, Du RL, She Y, Liu X. Kinetic analysis of tar's separation from
365 lump Coal[J]. The Iron and Steel Institute of Japan, 2015, 55(5):947-951.

366 [24] Wang T, Li C, Zhou BX, et al. Experimental investigation of thermal effect in
367 coal pyrolysis process[J]. Fuel Processing Technology, 2020, 200:106269.

368 [25] Wang YP, Zhang YF, Zhou Q, et al. Thermal kinetics analysis of coal-gangue
369 selected from Inner Mongolia in China[J]. Journal of Thermal Analysis and
370 Calorimetry, 2018, 131(2):1835-1843.

371 [26] Lv S, Lv GJ, Jiang XG, et al. Pyrolysis/combustion characteristics and kinetic

372 analysis of Indonesia lignite sludge[J]. Journal of China Coal Society, 2014, 39(3):
373 554-561.

374 [27] Ankit A. Jain, Anurag Mehra, Vivek V. Ranade. Processing of TGA data: analysis
375 of isoconversional and model fitting methods[J]. Fuel, 2016, 165:490-498.

376 [28] Ma YY, Ma Fy, He F, et al. Influence of microwave swelling with cavitated
377 creosote oil on the direct liquefaction performance of Xigou coal from Xinjiang and
378 its dynamics analysis[J]. Journal of China Coal Society, 2017, 42(10): 2733-2741.

379 [29] Czajka K, Kisiela A, Morón W, Ferens W, Rybak W. Pyrolysis of solid fuels:
380 thermochemical behaviour, kinetics and compensation effect[J]. Fuel Processing
381 Technology, 2016,142:42-53.

382 [30] Skodras G, Nenes G, Zafeiriou N, Low rank coal-CO₂ gasification: experimental
383 study, analysis of the kinetic parameters by Weibull distribution and compensation
384 effect[J]. Applied Thermal Engineering, 74 (2015), 111-118.

385 [31] Marbán G, Laura Río. Tentative explanation for the kinetic compensation effect
386 in doped catalysts[J]. Kinetics and Catalysis, 2013, 54(4):487-492.

387 [32] Meng DX, Wang T, Xu JL, Chen XL. Diffusion effect and evolution of kinetic
388 parameters during coal char-CO₂ gasification[J]. Fuel, 2019, 255, 115819.

389 [33] Rasam S, Haghghi A M, Kolsoom A, et al. Thermal behavior, thermodynamics
390 and kinetics of co-pyrolysis of binary and ternary mixtures of biomass through
391 thermogravimetric analysis[J]. Fuel, 2020, 280, 118665.

Figures

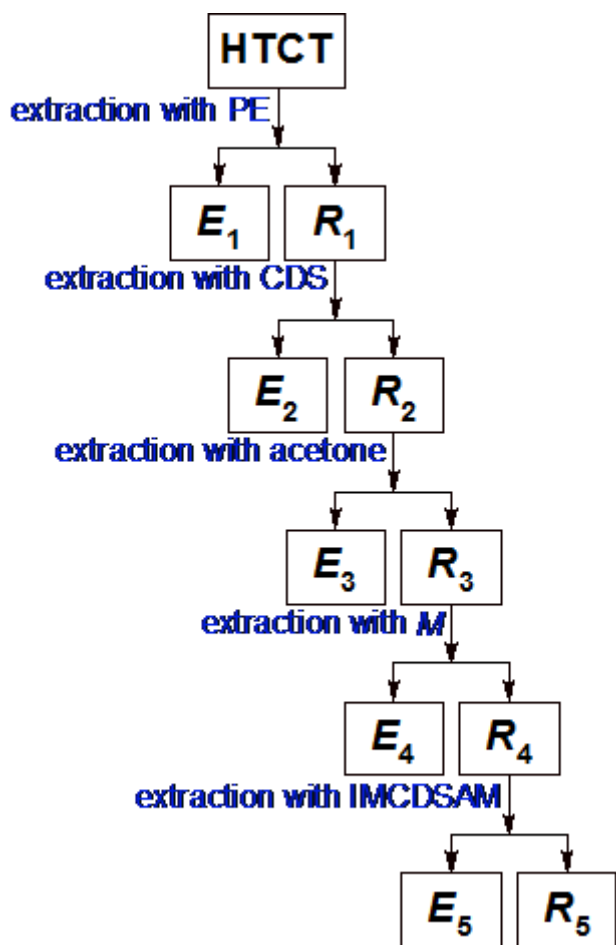


Figure 1

Sequential extraction process of HFAC.

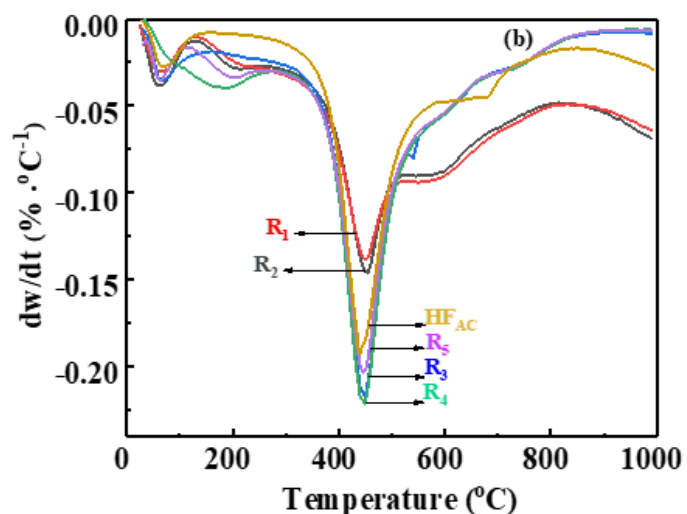
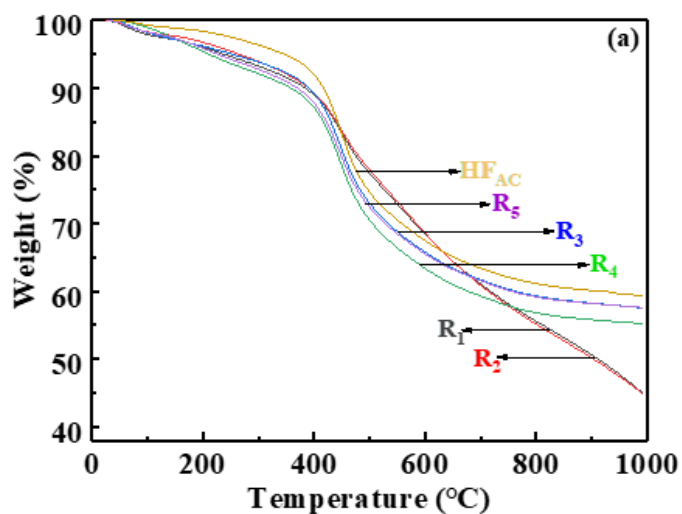


Figure 2

TG-DTG diagram of HFAC and its extract residues

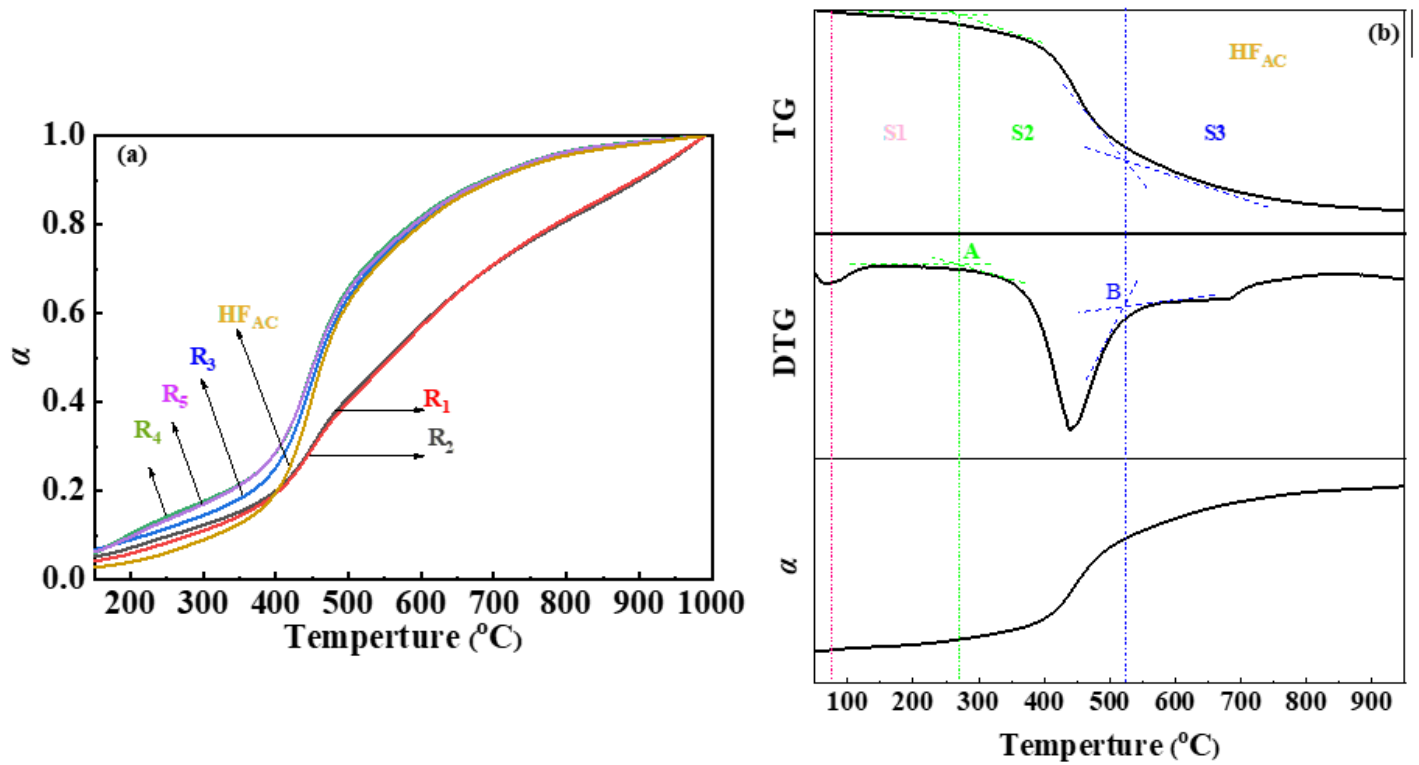


Figure 3

Diagram of conversion to temperature. (a): α -T ; (b): TG/DTG/ α -T

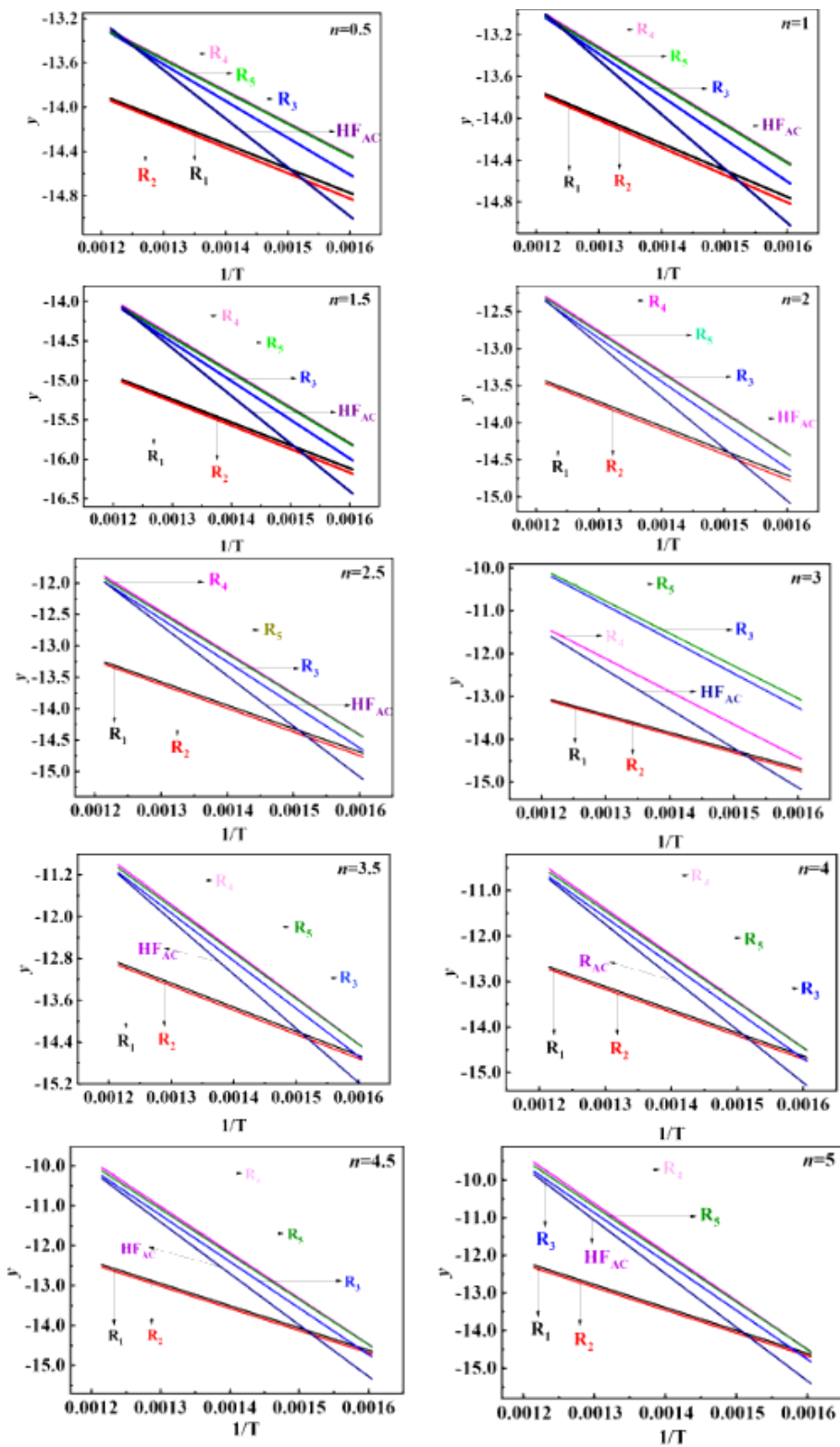


Figure 4

Fitting curves of each sample with reaction order $n=0.5-5$.

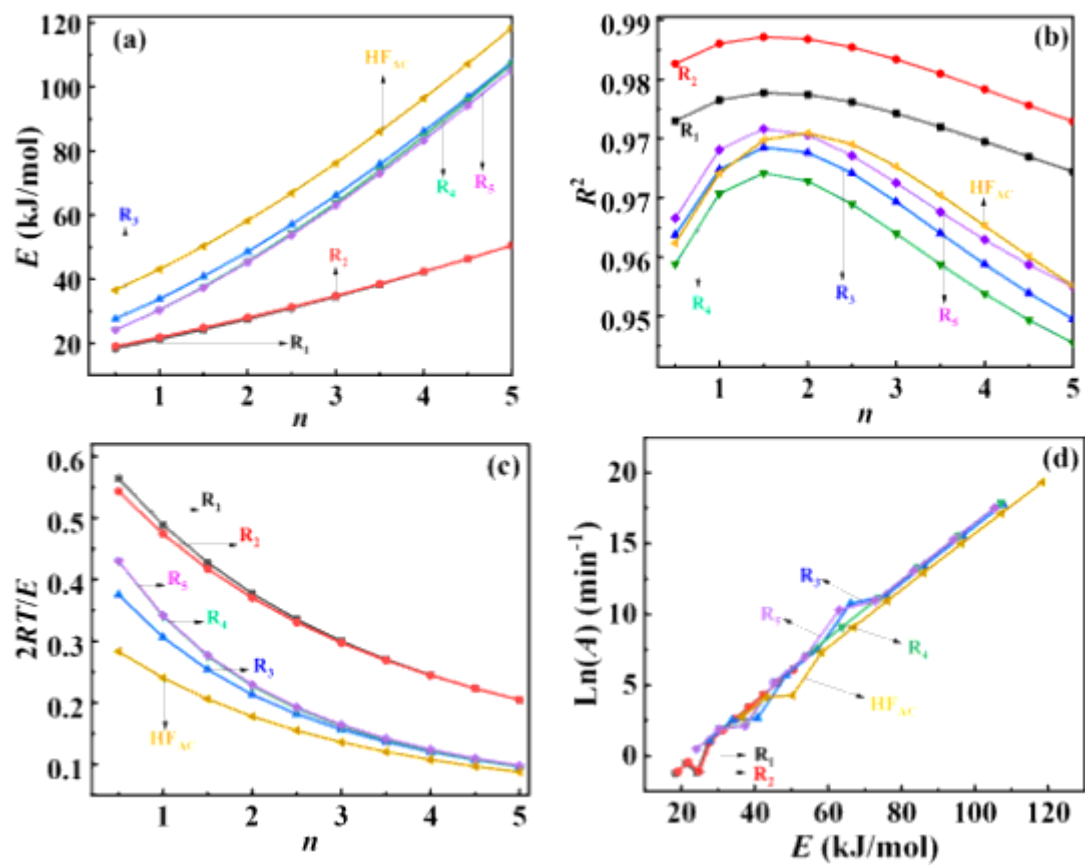


Figure 5

Relationship between kinetic parameters and reaction order.